molecular pharmaceutics

Article

pubs.acs.org/molecularpharmaceutics

Gellan Nanohydrogels: Novel Nanodelivery Systems for Cutaneous Administration of Piroxicam

Umberto M. Musazzi,[†] Claudia Cencetti,[‡] Silvia Franzé,[†] Nicole Zoratto,[‡] Chiara Di Meo,[‡] Patrizia Procacci,[§] Pietro Matricardi,[‡] and Francesco Cilurzo*[,†]

[†]Department of Pharmaceutical Sciences, University of Milan, via Giuseppe Colombo, 71, 20133 Milan, Italy

[‡]Department of Drug Chemistry and Technologies, "Sapienza" University of Rome, Piazzale Aldo Moro 5, 00185, Rome, Italy

[§]Department of Biomedical Sciences for Health, University of Milan, via Giuseppe Colombo, 71, 20133 Milan, Italy

Supporting Information

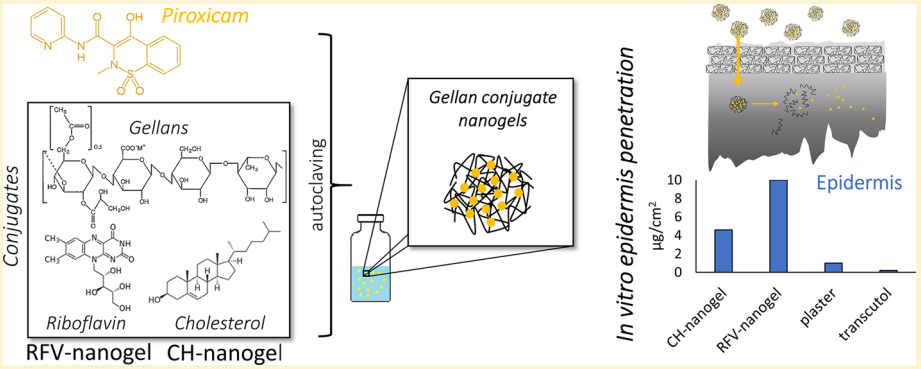

ABSTRACT: The feasibility to use gellan nanohydrogels (Ge-NH) as delivery system for the cutaneous administration of piroxicam (PRX) was investigated using gellan conjugated with cholesterol or riboflavin. The *in vitro* skin penetration studies through human epidermis were performed using a saturated aqueous drug solution, a 50% w/v Transcutol aqueous solution, and a commercially available PRX plaster as controls. Confocal microscopy, ATR-FTIR spectroscopy, circular dichroism, and a dynamometer assisted extrusion assay were performed to clarify the permeation mechanism of Ge-NHs. The skin permeation studies evidenced that Ge-NHs enhance the PRX retention in the epidermis and, at the same time, slow down the permeation process with respect to the controls. NHs can penetrate the *stratum corneum*, and then gradually disassemble thus diffusing in the viable epidermis reaching the spinosum layer. In conclusion, NHs represent a novel strategy to target poorly permeable compounds in the epidermis, thus improving the management of cutaneous pathologies.

KEYWORDS: *nanohydrogel, gellan, self-assembling polysaccharide, piroxicam, skin penetration*

INTRODUCTION

Nanosize hydrogels (nanogels, NHs) are polymer nanoparticles with three-dimensional networks, formed by chemical and/or physical cross-linking of polymer chains. Various nanogels have been designed as drug-delivery systems (DDS) and studied for different biomedical applications, such as regenerative medicine and bioimaging applications.[1−4]

Very recently, the feasibility to administer a drug in the skin by the use of nanogels has been also proposed.[5−8] Indeed, having a highly porous structure with a large water content, NHs seem to be able to enhance the skin penetration of the embedded (mainly hydrophobic) compounds. As an example, Smejkalova and co-workers found a significant increase of the retention of a hydrophobic probe (i.e., nile red) both in epidermis and in dermis using a nanogels obtained from an esterified hyaluronic acid.[9] In another work, the nano-encapsulation of ibuprofen into a ternary complex with chitosan and gellan significantly increased the permeation of the drug with respect to the control hydrogel.[10] Analogously, the permeation of acitretin through pig ear skin was improved by chitin base nanogels.[5] The skin permeation profile can be further optimized by using stimulus responsive nanogels as demonstrated in the case of caffeine.[11]

The permeation mechanism of nanogel through the skin has not been yet completely clarified, and, basically, two different hypotheses are reported in the literature. According to the first one, the enhancement effect may be related to the softness and physicochemical stability of the nanogel as suggested in the case of polyglycerol-based nanogels.[12] Alternatively, a loss of nanogel integrity with skin depth and a copenetration of nanogel components and their payload has been suggested.[9]

Received: October 24, 2017
Revised: December 21, 2017
Accepted: January 24, 2018
Published: January 25, 2018

DOI: 10.1021/acs.molpharmaceut.7b00926
Mol. Pharmaceutics XXXX, XXX, XXX−XXX

In order to further support the efficacy of physically cross-linked nanogels in enhancing the skin penetration of drugs, providing more information on the mechanism aspects, this work aimed to explore the feasibility of gellan based nanohydrogels (Ge-NHs) to deliver piroxicam (PRX) in human epidermis.

The feasibility to obtain Ge-NHs by using an innovative, reproducible process based on a standard autoclave cycle and the physicochemical stability of the resulting systems have been already demonstrated.[13−16] NH formation results from the self-assembling of Ge-cholesterol (GeCh) and Ge-riboflavin (GeRfv) derivatives, and hydrophobic drugs can be easily loaded within Ge-NHs.[14] PRX appears of particular interest as model drug since it is a very poorly permeable compound if compared to the other nonsteroidal antinflammatory drugs[17] and it has been proposed for the treatment of nonmelanoma skin cancers.[18,19]

Due to the risk of serious gastrointestinal adverse effects in comparison to other NSAIDs,[20,21] the development of a therapeutic system able to enhance the PRX retention in the skin, reducing at the same time the systemic exposure, may be beneficial to improve the safety of the treatment.

In the present work, the *in vitro* permeation profiles through human epidermis of PRX-loaded GeCh-NHs and GeRfv-NHs were investigated. Aiming to better understand their possible application in the design of drug delivery systems intended for cutaneous applications, their penetration patterns were compared to those obtained with a PRX saturated aqueous solution, PRX Transcutol aqueous solution, and a commercially available medicated plaster. The solutions were selected as reference to determine how the penetration profile of PRX was influenced by the drug loading in the nanohydrogel. In particular, Transcutol was used since it is a well-known skin penetration enhancer which favors the retention in the skin.[22] The medicated plaster was selected to better understand how efficient were Ge-NHs in enhancing drug permeation with respect to a drug product already authorized for the market for the treatment of locoregional painful syndromes.

EXPERIMENTAL SECTION

Materials. Piroxicam (PRX) was purchased from Cameo Healthcare (Thane, India). Egg phosphatidylcholine (Egg-PC) was kindly provided by Lipoid (Steinhausen, Switzerland). Tween 80 was obtained from Croda chocques (France); HPLC-grade, acetonitrile, and MeOH were purchased from VWR International PBI s.r.l. (Milan, Italy). Gellan (Ge) (Kelko product) was purchased from Giusto Faravelli (Italy). Cholesterol (Ch) and riboflavin (Rfv) were Sigma-Aldrich Srl (Milan, Italy) products. Transcutol (diethylene glycol monoethyl ether) was obtained from Gattefossé Italia (Milan Italy). All other reagents and solvents were purchased from Sigma-Aldrich Srl (Milan, Italy) and used without further purification.

Synthesis of Cholesterol- and Riboflavin-Conjugated Gellans. The high molecular weight native Ge (sodium salt form) was, at first, modified in the tetrabutylammonium salt form by ion-exchange resin. To obtain NHs, it is necessary to lower the M_W of the polymer. To this aim, Ge was extruded through an orifice at high pressure conditions (M-110EH Microfluidizer Processor in an extrusion chamber G10Z, 87 mm; P 1200 bar, T = 50 °C). A final $M_W \approx 2.75 \times 10^5$ determined by GPC was obtained.[13]

As a general method, the Ge derivatives were obtained by esterifying the polymer chains with a hydrophobic moiety, previously derivatized using an appropriate spacer according to a previously described reaction. Gellan-cholesterol (GeCh) was obtained by linking cholesterol (esterified with 4-bromobutyric acid; Ch) to the polymer chains in *N*-methyl pyrrolidone (derivatization degree, 9% mol/mol).[13] Gellan-riboflavin (GeRfv) was obtained by linking riboflavin tetrabutyrate (functionalized with 1,6-dibromohexane, Rfv) to the polymer chains (derivatization degree, by feed ratio, 30% mol/mol) according to the reaction already described in the literature.[15] Polymer derivatives were characterized according to procedures already described.[23] Moreover, FTIR spectra (4000−650 cm^{-1}) showed for both the samples a peak at about 1750 cm^{-1}, indicating the formation of the ester linkage between Ge and the hydrophobic moieties (Figure S1).

Preparation of Nanogels. The NHs were prepared by the autoclave process as previously reported.[14,15] Briefly, 3.0 mg of each gellan derivative (i.e., GeCh or GeRfv) were dispersed in 3.0 mL of distilled water (1.0 mg/mL) by overnight magnetic stirring at 25 °C. At the same time, 1 mL of PRX acetone solution (2 mg/mL) was added to a glass vial and stored at room temperature until the complete solvent evaporation, thus forming a film of the drug. The Ge derivate suspension (3 mL) was then added to this vial, shaken in vortex, and autoclaved for 20 min at 121 °C and 1.10 bar (Autoclave-steam sterilizer 2440 ML, Tuttnauer, NL). At the end of the process, a PRX-loaded NH suspension was obtained. The resulting suspension was withdrawn and centrifuged at 20 °C, 4000 rpm, 10 min (Universal 30RF, Hettich Zentrifugen, Germany). The supernatant containing NHs was stored for further studies. Blank NHs were prepared as well following the same protocol. The PRX chemical stability to the autoclaving process was preliminary evaluated by the HPLC method reported below.

Particle Size and ζ-Potential Measurements. The mean hydrodynamic diameter of NHs (D_h), PDI, and ζ-potential were measured at 25 °C by the DLS method. Aliquots of supernatant containing NHs were diluted 1:10 in HPLC-grade water and analyzed by Zetasizer Nano ZS (Malvern Instruments Ltd., U.K.).

Drug Content. The PRX amount loaded in the NHs was determined indirectly as follows. After the centrifugation step above-described, the pellet was solubilized in 2 mL of ethanol to extract the unloaded amount of PRX. At the same time, the vial used for autoclave cycle was cleaned with 2 mL of ethanol to recover the PRX absorbed on the wall. The two ethanolic solutions were mixed and diluted 1:20 in the mobile phase described below to determine the PRX amount unloaded. The amount of the loaded drug was determined by subtracting the result from the amount of PRX initially added to the vial.

Absorption Spectrum of PRX. The determination of maximum peak of absorbance (λ_{max}) of PRX loaded in the NHs was performed using a UV−vis spectrometer Lambda 25 (PerkinElmer, USA). Before the analyses, the drug-loaded NH suspension was diluted 1:10 in HPLC-grade water and, then, put in quartz cuvettes with a light path of 10 mm (Hellma Analytics, USA). The UV spectrum was recorded from 200 to 700 nm using HPLC-grade water as blank reference. The λ_{max} was graphically determined from the resulting UV spectrum of the sample. Saturated PRX aqueous solution and PRX solutions (20 μg/mL) in acidified (0.125 M phosphate buffer sodium pH 2.0, Eur.Ph. 9.0; pH = 2) and alkaline conditions (0.1 M phosphate buffer solution, Eur.Ph. 9.0; pH = 10) were used as controls.

DOI: 10.1021/acs.molpharmaceut.7b00926
Mol. Pharmaceutics XXXX, XXX, XXX−XXX

Mechanical Properties of Nanogels. The ability of NHs to act as soft carriers, squeezing through the narrow intracellular spaces of the packed *stratum corneum*, was assessed by a dynamometer assisted extrusion process, according to the method previously developed for studying the deformability of flexible liposomes.[24] Briefly, samples of Ge-NHs were diluted to a concentration of 0.05 mg/mL in Milli-Q water and loaded in 1 mL gastight syringe, held with the needle facing downward into an extruder casing fixed to a vertical holder. The syringe plunger was put in touch with a 50 N load cell of a dynamometer (INSTRON 5965, ITW Test and Measurement Italia Srl, Italy) set up to move the plunger at a constant rate of 1 mm/s, forcing NH suspension through a polycarbonate membrane, pore diameter 50 nm. To minimize the dead volume and to carry out the test correctly, the membrane was prewetted with Milli-Q water before each test. At the end of the experiment the extruded fraction was collected and analyzed by DLS for particle size determination and counting of the particles. The force (N) required to extrude the NH suspension through the membrane was registered as a function of the plunger displacement (mm), and the constant of deformability (k) was calculated as the slope of the resulting curve.[24] A highly flexible transferosome formulation, made of Egg-PC and Tween 80 (85:15 w/w %) and prepared by the thin film hydration method, was used as a reference.

Quantification of Piroxicam by HPLC. The concentration of PRX was determined by HPLC (HP 1100, ChemStations, Agilent Technologies, USA). Separation was carried out using a reverse-phase column (LiChrospher 100 RP-18E, 5 μm, 125 × 4.0 mm, CPS Analitica, Italy) and 0.03 M phosphate pH 3.0 buffer/acetonitrile (60/40% v/v) as mobile phase. The flow rate was 1.5 mL/min, and the injection volume was 20 μL. The retention time of PRX was 2.4 min. The drug concentration was determined at two wavelengths (i.e., 248 nm, 360 nm) from calibration curves in the range of 0.05−20 μg/mL (R^2 > 0.999).

***In Vitro* Skin Permeation Experiments.** The permeation studies were performed using the frozen abdominal skin from three different donors, who underwent cosmetic surgery within one month before the *in vitro* experiment. Epidermis samples were prepared following an internal standard procedure.[25] The full-thickness skin was sealed in evacuated plastic bags and frozen at −20 °C within 6 h after removal. Before the experiments, the skin was thawed at room temperature, and the excess of fat was carefully removed. The skin sections were cut into squares of about 4.9 cm^2, and, after immersion in water at 60 °C for 1 min, the epidermis was gently separated from the remaining tissue with forceps. The electrical resistance (R) of the isolated epidermis was measured to ensure the integrity of the barrier membrane, and epidermis samples with R values above 25 kΩ cm^2 were used for experiments (voltage, 100 mV; frequency, 100 Hz; Agilent 4263B LCR Meter, Microlease, I). The epidermis sample was mounted on the Franz diffusion cell with a permeation area of 0.636 cm^2. The receptor compartment (volume: ≈ 3.0 mL) was filled with 0.9% w/v NaCl aqueous solution containing 100 μg/mL NaN_3 as preservative. The receptor phase was selected to guarantee the sink condition throughout the permeation experiments. Special care was given to avoid air bubbles between the buffer and the epidermis in the receptor compartment. The upper and lower parts of the Franz cell were sealed with Parafilm (Pechiney Plastic Packaging Company, USA) and fastened together by means of a clamp, with the epidermis acting as a seal between the donor and receptor compartments. Then, the donor compartment was filled with 0.4 mL of tested liquid formulations. The system was kept at 37 °C using a circulating water bath, so that the epidermis surface temperature was at 32 ± 1 °C throughout the experiment. At predetermined time intervals (1, 4, 6, 16, 24 h), 200 μL samples were withdrawn from the receiver compartment and replaced with a fresh aliquot of receiver medium. Samples were analyzed by HPLC according to the method described in the dedicated section. Moreover, in the case of GeRfv-NHs, the withdrawn aliquots were also analyzed using a Wallac 1420 Victor2Microplate Reader (PerkinElmer, US) to estimate the permeation pattern of the GeRfv. The excitation and the emission wavelengths were set at 355 and 535 nm, respectively. The values are expressed as the average of parallel experiments performed at least in duplicate using an epidermis sheet from each of the three donors (n = 6). The cumulative amount permeated through the skin per unit area (Q_i) was calculated from the drug concentration in the receiving medium and plotted as a function of time. The maximal flux (J_{max}) was determined as the slope of the linear portion of the plot Q_i vs time (R^2 > 0.98).

At the end of the permeation experiments, the concentration of PRX retained in the epidermis (R_{24}) was quantified by the following procedure. The epidermis sheet was removed from the Franz diffusion cell, and each side was gently treated with 5 mL of methanol (MeOH) to wash out the unabsorbed drug. Subsequently, the sample was dried, thinly sliced, and placed in 5 mL of fresh MeOH. The suspension was soaked in a sonicator for 30 min and then maintained for 24 h at 2−8 °C. Finally, the supernatant was filtered through a 0.45 μm filter and analyzed by HPLC. R_{24} was expressed as micrograms of PRX per square centimeter.

The R_{24}/Q_{24} ratio was used to underline the PRX affinity for the epidermal layers and the influence of the formulation on such paramenter.[26]

The performances of the NHs in terms of skin permeation were assessed using a PRX saturated aqueous (16 μg/mL) solution, 500 μg/mL PRX in a Transcutol aqueous solution (50% w/v), and a medicated plaster already available on the Italian market (PRX content 200 μg/cm^2; Brexidol, Promedica Srl, Italy). In this case, the experimental protocol was slightly modified: despite liquid formulation, the plaster was attached on the human epidermis immediately before the membrane was mounted on the Franz diffusion cell.

Attenuated Total Reflection (ATR) Spectroscopy. Epidermis samples were prepared following an internal standard procedure as described above. 24 h before the ATR analyses, each epidermis sample was put in a Petri dish and 2.0 mL of 1 mg/mL NH aqueous dispersion was added at the interface with the *stratum corneum*. An aliquot of Milli-Q grade water was used as control. The samples were stored at room temperature for 24 h. At the end of incubation time, each sample was carefully cleaned to eliminate the solution residues on the surface and, then, dried at room temperature for 30 min before ATR analyses. Afterward, each sample was carefully wiped with filter paper and let equilibrate for 15 min at 23 °C and 50% RH before testing. FTIR measurements were performed using a SpectrumOne spectrophotometer (PerkinElmer, USA), by placing the epidermal sample on a diamond crystal mounted in an ATR cell (PerkinElmer, USA). The spectra were collected over the wavenumber region 4000−650 cm^{-1} at 4 cm^{-1} resolution and 128 scans. The raw data were elaborated by ATR correction (Spectrum, PerkinElmer, USA);

DOI: 10.1021/acs.molpharmaceut.7b00926
Mol. Pharmaceutics XXXX, XXX, XXX−XXX

the band maxima were assigned by second derivative after smoothing with a seven-point Savitsky−Golay function using Originlab 2015.

Circular Dichroism (CD). To detect possible interaction between the Ge derivatives and keratins in the *stratum corneum*, CD spectra were recorded using regenerated keratin as model compound. The protein was obtained by wool using the protocol described by Selmin and co-workers.[27] CD spectra were recorded on a J-810 spectropolarimeter, using a quartz cuvette of 0.1 cm path length, between 190 and 260 nm at a scanning rate of 50 nm/min with 0.5 nm resolution. The analyses were carried out on 0.1 mg/mL samples in water at room temperature.

Confocal Microscopy Analysis. Samples from *in vitro* permeation experiments were embedded in OCT compound (Miles Laboratories, Elkhart, IN, USA), rapidly frozen in liquid nitrogen, and stored at −80 °C, pending sectioning. Cryostat sections (15 μm thick), cut from frozen skin samples, were collected on adhesive coated slides, air-dried, and stored at −20 °C until use.

For confocal microscopy analysis, sections were rehydrated in PBS 0.1 M and stained with 4′,6-diamidino-2-phenylindole (DAPI), Sigma-Aldrich Srl (Milan, Italy), to label nuclei. After final washing, sections were mounted with Mowiol mounting medium Sigma-Aldrich Srl (Milan, Italy).

Sections were examined with a confocal microscope Zeiss LSM 510 system (Gottingen, Germany).

Images from different slices were obtained through a 40× oil immersion objective at 1024 × 1024 pixel resolution, and acquired with the software A.I.M. 4.2.

RESULTS

Characterization of Nanogels. The two prepared NHs, based on GeCh and GeRfv, had similar physicochemical characteristics. Indeed, D_h were 177 ± 28 and 178 ± 16 nm for GeCh-NHs and GeRfv-NHs, respectively. The ζ-potential was close to −40 mV in both cases, determining a good physical stability in water. The PRX was uploaded within the NHs by autoclaving a suspension of the drug in the presence of the Ge derivatives. The PRX content resulted as 282 ± 31 μg/mg and 301 ± 12 μg/mg, respectively. It is worth noticing that the more general mechanism of the uploading of hydrophobic drugs within the NHs is not yet clearly elucidated. As described in a previous paper,[16] the mechanism could be related to the hydrophobic interactions among the drug molecules and the hydrophobic moieties responsible of the NH assemblies. These interactions could be favored by the high temperature reached during the autoclave treatment. It should be also emphasized that the preparation method led to obtaining NH suspensions in which the drug was mainly loaded into the nanogel, but also partially free in the suspension medium, which resulted as saturated, avoiding the drug leakage from the nanocarrier. In addition, the results obtained by UV analyses highlighted that the encapsulation of PRX in NHs did not alter its ionization equilibrium since the λ_{max} of both saturated solution and PRX-loaded GeCh-NHs resulted as superimposable (Table 1). The tests were performed only on GeCh-NHs, as the λ_{max} of GeRfv interfered with the absorbance spectrum of PRX.

Moreover, the obtained λ_{max} values were comparable to that obtained at pH 10, suggesting that PRX was in the zwitterionic/anionic form. Indeed, it is noteworthy that the λ_{max} of PRX varies as a function of the ionization state of the molecule.[28] At acidic pH values, the pyridine moiety, that is part of the PRX structure, results to be protonated. When the pH increases above 7, the deprotonation of pyridine moiety induces a bathochromic shift of λ_{max}. Although the PRX anionic form prevails at high alkaline pH, the stabilization of a planar conformation of PRX due to the intramolecular hydrogen bond between the pyridine and the carbonyl group permits the formation of zwitterion. With respect to the experimental data, the existence of PRX zwitterionic form was also suggested by the yellowish color observed in the case of the saturated PRX solution.[29]

Table 1. Maximum Peak of Absorbance of PRX in Nanogels and Reference Solutions

formulation	solvent	λ_{max} (nm)
satd PRX soln	water	358
PRX-loaded GeCh-NHs	water	357
PRX soln pH 2	acidified water (pH = 2)	343
PRX soln pH 10	alkaline water (pH = 10)	354

***In Vitro* Skin Permeation Experiments.** The permeation profile of saturated PRX solution resulted to be negligible (Table 2; Figures S2, S3), despite the R_{24} value suggesting that PRX penetrates the *stratum corneum*. Indeed, it is noteworthy that the low drug solubility in water strongly influences the permeation process, affecting the concentration gradient among the membrane layers. On the contrary, the PRX content in the medicated plaster induced a 25-fold increase of the amount of the drug loaded in the donor compartment with respect to the saturated solution. In these conditions, the PRX significantly permeated through the human epidermis, as demonstrated by the resulting flux value and the retained amount (Table 2; Figures S2, S3). However, Q_{24} and R_{24} were 1.04 ± 0.28% and 0.52 ± 0.14% of the applied dose respectively, confirming the limited poor tendency of PRX to permeate through the skin.

When NHs were used as drug carriers, the R_{24} values obtained after the application of NHs significantly increased with respect to the reference formulations (Table 2, p-value <0.05). Moreover, the permeation process was slowed down in comparison to medicated plaster (Q_{24}, J_{max}, lag time, p-values <0.001). Independently of the composition of the NHs, a slight increase of the "PRX utilization" of the dosage form with respect to the medicated plaster was recorded. In agreement with the EMA Guideline on quality of transdermal patch (EMA/CHMP/QWP/608924/2014), the PRX utilization was defined as the percentage of total drug absorbed within the entire *in vitro* experiment with respect to the initial drug loading of the dosage form. Indeed, the PRX utilization of the medicated plaster was ≈1.5% while that of the NHs resulted at least 2-fold higher. In particular, GeRfv-NHs appeared to be the most efficient formulation with respect to the R_{24} expressed both as absolute value (Table 2) and as percentage (i.e., 5.59 ± 2.03% of the applied dose). In addition, the dose-normalized permeation results showed that GeRfv-NHs was effective in minimizing the drug permeation through the human epidermis (i.e., 0.03 ± 0.01%). The capability of NHs to promote the PRX retention within the human epidermis was also confirmed by the comparison of the R_{24}/Q_{24} values (Table 2). If the plaster value was bias for the permeation through the skin (R_{24}/Q_{24} = 0.5), the R_{24}/Q_{24} was strongly in favor of the numerator of the fraction for all the NH formulations (R_{24}/Q_{24} > 20). This resulted in a GeRfv-NHs ratio 10 times higher than GeCh-NHs.

DOI: 10.1021/acs.molpharmaceut.7b00926
Mol. Pharmaceutics XXXX, XXX, XXX−XXX

Table 2. Results of *in Vitro* Permeation Studies on PRX-Loaded GeCh-NHs, GeRfv-NHs, PRX 50% w/v Transcutol Solution, and Saturated Solution and Plaster (Mean Value ± SD; $n = 6$)

formulation	PRX dose ($\mu g/cm^2$)	Q_{24} ($\mu g/cm^2$)	lag time (h)	flux ($\mu g/cm^2/h$)	R_{24} ($\mu g/cm^2$)	R_{24}/Q_{24}
GeCh-NHs	146	0.221 ± 0.107	7 ± 4	0.018 ± 0.005	4.626 ± 1.237	21
GeRfv-NHs	189	0.049 ± 0.020	>16	–[a]	10.290 ± 3.743	210
satd soln	8	–	>24	–	0.031 ± 0.053	–
50% w/v Transcutol soln	200	0.436 ± 0.167	>16	–[a]	2.391 ± 0.835	11
plaster	200	2.07 ± 0.551	3 ± 0	0.100 ± 0.024	1.033 ± 0.275	0.5

[a]The flux was not calculated since the long lag time.

Based on the obtained results, the GeRfv-NHs, which resulted as the most effective formulation in enhancing the localization of PRX in the skin, was thus selected to study the penetration pattern.

Confocal Microscopy Images. The pattern of penetration of the GeRfv-NHs within the human epidermis was followed by confocal microscopy, taken advantage of the autofluorescence of riboflavin. Images were recorded on skin samples exposed to the GeRfv-NHs for different times (1, 2, 4, 6, 24 h; Figure 1). Nuclei of the epidermal cells appear as bright blue ovals. In control samples (not shown) any green signal was evident.

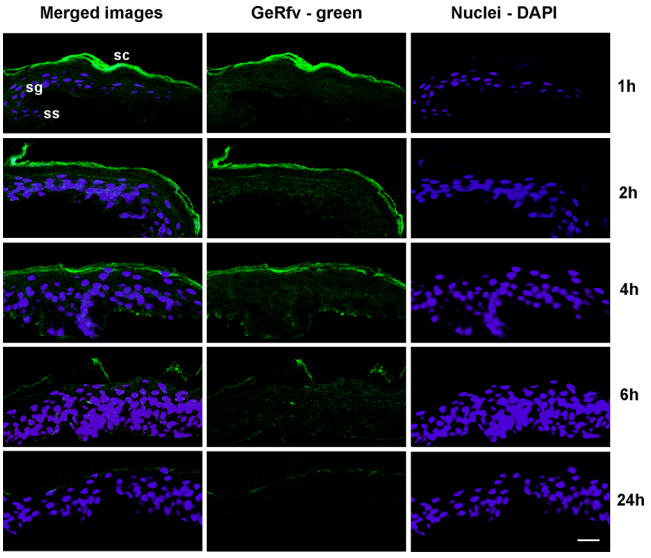

Figure 1. Confocal images obtained from frozen skin samples treated by GeRfv-NHs. Merged images show green signal detection on the outer surface of the skin and in the deeper layers at different times points after the treatment. Green fluorescence is due to the GeRfv. Nuclei are stained blue with DAPI. SC = *stratum corneum*; SG = *stratum granulosum*; SS = *stratum spinosum*. Images were acquired under a 40× oil immersion objective. Scale bar = 20 μm.

As depicted in Figure 1, after 1 h of exposure, NHs concentrate mainly on the outer skin surface, remaining essentially confined in the *stratum corneum*, while a weak fluorescence is noticed in the epidermal layers, mainly at the granulosum–spinosum limit (after 2 h). The probe signal, detected on the outer surface of the skin, underwent a significant reduction over time until it almost disappeared after 24 h after the initial treatment. This seems to be related to the diffusion of the probe deeper in the epidermis layers, up to the spinosum layer. Indeed, after 6 h exposure to GeRfv-NHs a homogeneous green fluorescent signal was observed throughout the epidermis, suggesting a great affinity of the polysaccharide scaffolding of the gel for the skin components. Finally, it should be mentioned that the fluorescence of GeRfv-NHs in the receiving medium of the Franz cell after 24 h experiment was not significantly different from the fluorescence of the samples exposed to untreated epidermis samples, suggesting a negligible GeRfv permeation through the human epidermis.

Mechanical Properties of Nanogels. Nanosized channel-like pores of the stratum corneum are one of the major pathways suggested for the skin penetration of nanocarriers,[9] and, therefore, the ability of the delivery systems to squeeze through these pores is a requirement for the release of the drug payload deep into the skin. Nanogels are highly porous, soft, and compressible materials, since they can exchange water with the external environment undergoing swelling and deswelling processes. Therefore, they could adapt their structure thus crossing the tight skin barrier. In this respect, Montanari et al. found that HA based nanogels exhibit a low Young's modulus as determined by AFM analysis.[16] Moreover, Hendrickson and Lyon reported the first proof of concept that nanogels, after application of a pressure, can undergo such a deformation to pass through cylindrical pores having a diameter one tenth smaller than their own diameter.[30] Basing on this evidence, we investigated the behavior of our NHs during constriction passage through track-etch membranes having pores at least 3.5 times smaller than their own size to resemble the penetration through the nanoporous structure of the *stratum corneum*. The test was performed at constant rate to estimate the forces acting during this process. In Figure 2, a representative curve obtained after extrusion of the NHs is reported.

After the first peak, which corresponds to the force required to overcome the frictions for plunger displacement, the force

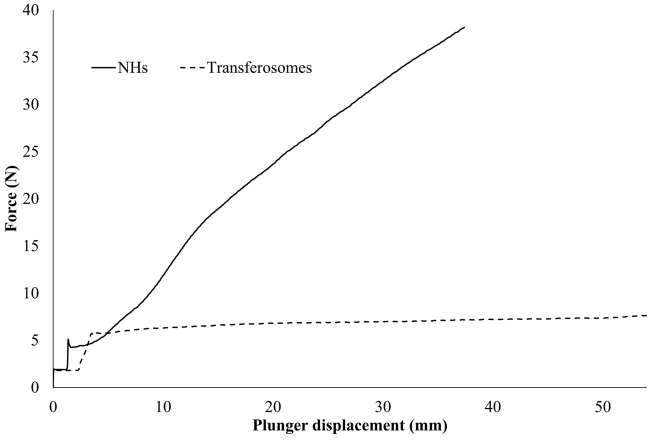

Figure 2. Representative curves of the force versus plunger displacement registered forcing GeRfv-NHs through 50 nm polycarbonate membranes (solid line) and transferosomes (dashed line).

DOI: 10.1021/acs.molpharmaceut.7b00926
Mol. Pharmaceutics XXXX, XXX, XXX–XXX

Table 3. ATR-FTIR Data of Human Epidermis Samples Treated with GeCh-NHs and GeRfv-NHs[a]

	stretching CH_3		stretching CH_2				
epidermis treatment	symmetric	asymmetric	symmetric	asymmetric	$H_{2920/2850}$	scissoring CH_x	fwhm
control	2958.0 ± 0.1	2923.5 ± 0.1	2873.3 ± 0.1	2854.1 ± 0.1	1.841.0 ± 0.1	1466.4 ± 0.1	12.1 ± 0.3
GeCh-NHs	2958.1 ± 0.1	2923.2 ± 0.1	2873.4 ± 0.1	2854.0 ± 0.1	1.783.0 ± 0.0	1466.5 ± 0.0	12.8 ± 0.8
GeRfv-NHs	2957.8 ± 0.3	2923.1 ± 0.1	2873.2 ± 0.1	2854.1 ± 0.1	1.801.0 ± 0.0	1466.6 ± 0.1	13.6 ± 0.3

[a]Epidermis samples treated only by water were used as a control.

progressively increased until the maximum limit (based on the equipment performances) was reached determining the end of the test run. Only 2% of NHs were found in the filtrate and the particle size resulted reduced by about 40% of the initial particle diameter, suggesting that nanogels partially lost their structure during the passage through the pores, finally occluding the porous membrane. Indeed, the force versus plunger displacement curve registered for NHs did not present the plateau segment registered for transferosome suspension, which seems to freely flow through the membrane pores (Figure 2). Finally, the k value registered for the NHs (~0.9 N/mm) resulted to be 4-fold higher than that obtained for Egg-PC based transferosomes (~0.02 N/mm).

ATR-FTIR Spectroscopy and CD Measurements. The changes in the barrier properties of *stratum corneum* exposed to a chemical can be attributed to an alteration of the intercellular lipids from orthorhombic conformation toward the less ordered hexagonal conformation and/or the extraction of ceramides. These effects can be monitored by ATR-FTIR spectroscopy analyzing the possible shift of bands in the CH_x stretching region or measuring the CH_2 scissoring bandwidth (expressed as the full width at 50% peak height, fwhm).[31] The treatment of the human epidermis by nanogels did not determine any significant shift of CH_x stretching vibration bands (Table 3; Figure S3). Moreover, the fwhm values of the CH_2 scissoring bandwidth were in the 11.0−14.0 cm^{-1} range, confirming that all formulations did not affect the organization of lipids since they remained in the most stable orthorhombic conformation. This lack of alteration of lipidic network was further confirmed by the evaluation of the ratio between the heights of the band at about 2923 and 2853 ($H_{2920/2850}$) which, remaining almost constant after the treatment with NHs, excluded a possible extraction of lipids from the *stratum corneum*.

The analysis of the amide I and amide II regions confirmed the lack of significant interactions between the Ge-NHs and the main *stratum corneum* components. First, the treatment of epidermis sheet with Ge-NHs does not determine any modification of the maximum of the amide I that remained centered in the 1650−1660 cm^{-1} region, confirming that the main conformation of α-helical conformations prevails in the *stratum corneum* proteins (data not shown). Second, the ratio among the amide I and amide II height, which is an indication of protein unfolding,[32] remained almost constant. Third, the research of the amide I hidden peaks by second derivative evidenced the lack of any significant modification of the wavelengths, which overlapped those already described in the literature.[33] This wavenumber did not significantly change after the treatment by both of the formulations. This lack of significant modifications in keratin conformations is further confirmed by CD analyses performed on regenerated wool keratin which presents a prevalent α-helical conformation. Indeed, the CD spectra recorded on regenerated keratin and keratin GeCh mixtures overlapped and the small reduction of the intensity was attributed to dilution of the protein, as exemplified in Figure 3.

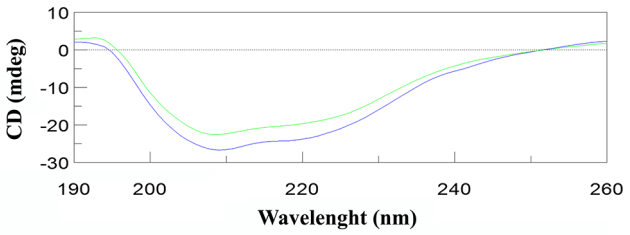

Figure 3. CD spectra of regenerated keratin (blue line) and regenerated keratin/GeCh 1/1 mixture (green line).

DISCUSSION

Ge-NHs represent a new useful tool in drug delivery for many reasons. The biocompatibility of Ge and the soft consistency of the NHs, due to the hydrogel structure at nanoscale, is a favorable environment for loading drugs in a well-tolerated device. Moreover, the innovative method for the NHs forming and loading in one shot by means of an autoclave, leading to a sterile suspension, is particularly appealing for a large-scale application of these nanodevices. Ge-NHs have been already exploited in loading and delivery of hydrophobic drugs, such as paclitaxel. In that case, the drug loading is allowed by the hydrophobic interactions between the drug molecules and the hydrophobic zones in the NHs, which are built up by the cholesterol moieties linked to the polymer chains. As can be easily argued, this property can be exploited for loading and delivery of many other hydrophobic drugs. Starting from the above-mentioned properties and taking into account the skin structure and the results described in the literature on the applications of nanodevices in topical drug delivery,[5,7,8] this work aims to demonstrate the usefulness of Ge-NHs also in cutaneous applications, improving the PRX administration through the skin. The PRX loading in Ge-NHs determined a modification of its skin penetration pattern with respect to a medicated plaster, which can be considered one of the most effective dosage forms to sustain the permeation of this model drug through the skin. Indeed, NHs enhanced the skin retention, R_{24}/Q_{24} values being significantly higher than those obtained by both the Transcutol solution and the PRX plaster. The same effect was also described in the case of clobetasol: the use of chitin nanogels that enhanced the skin retention with respect to a marketed cream.[7] The comparison with Transcutol is particularly interesting since this compound is claimed to increase the drug solubility in the skin and therefore its retention.

This data suggested that the effect of nanogels cannot merely be ascribed to an increase of the PRX apparent solubility. Indeed, a modification of the drug apparent solubility should influence only the partition of the permeant from the donor

DOI: 10.1021/acs.molpharmaceut.7b00926
Mol. Pharmaceutics XXXX, XXX, XXX−XXX

toward the *stratum corneum* while the subsequent processes (i.e., the diffusion through the epidermis layers and the partition toward the receiver medium) should resulted unaffected. Thus, assuming that the adhesive matrix of a patch acts as a drug reservoir on the skin,[34] the R_{24}/Q_{24} values obtained with the Ge-NHs and the medicated plaster should overlap. Moreover, the enhancement of the localization of PRX in the epidermis layer could not be ascribed to a change in the ionic equilibrium of PRX, as shown by the negligible differences between the UV spectrum of native PRX and drug-loaded GeCh-NHs. Such findings seem to demonstrate that Ge-NHs play an active role in the whole permeation process of PRX through the human epidermis. As clearly evidenced by confocal images, the green signal of Rfv was already detectable in the *stratum granulosum* after 1 h from the application. At time points of 2, 4, and 6 h the signal became detectable also in the *stratum spinosum*, even if weaker and more scattered. However, since the resolution confocal microscope cannot discriminate the presence of intact NHs into the epidermis, the generated data are unable to define if the Ge derivatives are able or not to penetrate the skin as intact NHs or disassembled during the penetration. Although these results are in agreement with other published ones,[6,7] no conclusive evidence was available regarding the penetration mechanism of nanogels.

It may be hypothesized that, once Ge-NHs are in contact with the skin environment, a modification of their inner structure may occur. Indeed, hydrophobic attractive forces between the hydrophobic moieties of Ge chains (i.e., cholesterol, riboflavin) stabilized the 3D structure of Ge-NHs from a critical value of concentration in water.[16] When such systems interact with the upper skin layers, the low water content (≈20%) of *stratum corneum* and the presence of the crystalline lipid matrix in the extracellular spaces[35] may induce a change of the interaction pattern within the spherical-like network of Ge-NHs. In particular, the lipidic matrix of the *stratum corneum* could interact with the hydrophobic moieties of Ge derivatives (i.e., cholesterol, riboflavin), reducing the cohesive forces between the polysaccharide chains and thus favoring their disassembly.

The low water content of *stratum corneum* could also drive a loss of water and a partial shrinkage of the swollen Ge-NHs. Moreover, most of the green signal associated with the Ge grafted riboflavin is localized in the *stratum corneum* and appeared uniformly distributed suggesting an affinity for keratin as already demonstrated for hyaluronan, which has a similar structure.[36] Thus, it is reasonable to hypothesize that the NH shrinkage and the possible interactions with keratins could trigger the disaggregation of the nanoassembly. This possibility is supported by the measurements of the ζ-potentials of regenerated keratin, Ge derivative, and their mixtures. As an example, the ζ-potential of 0.1 mg/mL regenerated keratin and GeCh solutions was -28.0 ± 1.1 mV and -39.6 ± 1.4 mV, respectively. Their 1:1 mixture resulted as -31.9 ± 2.4 mV, suggesting a possible weak interaction between the two components, which reduced the ζ-potential value of the polysaccharide derivative. This interaction should mainly influence the conformation of the Ge derivative since the CD spectra did not evidence any modification of the regenerated keratin and the ATR-FTIR spectra registered on the human epidermis did not evidence any significant modification of the conformation of skin proteins. This latter data appeared of interest since the unfolding of skin protein is generally considered an indication of the possible toxicity of the permeants.[32]

All of the above considerations supported the idea that the NHs favor the partition of PRX within the *stratum corneum* and the NH disassembly can favor the localization of the drug in the viable epidermis. The disassembly of the nanostructure could also be justified by the reduction of the intensity of the green signal in the confocal images of the epidermis layer over time. This hypothesis is in agreement with the results of FRET analyses performed on hydrophobic hyaluronic nanogels which suggested their significant disaggregation when they reach the viable epidermis.[9] Indeed, the nanogel did not present a sufficient deformability, as demonstrated by the extrusion assay, to penetrate the *stratum corneum* through the hydrophilic pathway similarly to deformable vesicle and their dimensions are too large for a diffusion through an intercellular route as in the case of metallic nanoparticles.[37] On the other hand, their Young modulus is quite similar to that reported for conventional liposomes, thus it was reasonable to hypothesize that, even if the structure is completely different, their behavior could be similar. Indeed, also in the case of conventional liposomes it is generally recognized that they enhance the drug retention into the skin disintegrating or fusing on the skin surface, thus exchanging lipid components with the *stratum corneum* and favoring the drug release.[38]

CONCLUSIONS

The literature has described the NHs as good drug carriers in many applications. The results obtained in the present work indicate that Ge-NHs can be useful in carrying and enhancing the skin penetration of insoluble and poorly permeable drug substances. Although their mechanism of action needs a deeper investigation, the obtained data suggest that they can penetrate intact in the upper skin layers and they experience a gradual disassembling process by the diffusion in the deeper epidermis layers. The ability of GeCh- and GeRfv-NHs to localize the drug in the epidermis along with the possibility to be internalized in epidermal cell lines makes such nanosystems advantageous in opening new therapeutic strategies in the management of cutaneous pathologies. Finally, it should be underlined that these formulations could be considered as the final dosage form to dermal delivery of drug molecules. Indeed, in a previous work, we demonstrate the feasibility to administer other nanocarriers, namely, ultraflexible liposomes and nanoemulsions, by a simple spray.[31,39] This approach should be advantageous since the nanogel suspension can be administered as such, avoiding dilutions that can reduce their concentration or can cause the diffusion of the loaded drug outside the nanocarrier. Indeed, the preparation method led to obtain a suspension in which the drug is both loaded in the nanogel and free in the suspension medium, which resulted as saturated, avoiding drug leakage from the nanocarrier. In the specific case of PRX, the permeation of the solubilized fraction through the human epidermis is negligible in comparison to the penetration pattern of PRX-loaded Ge-NHs, as demonstrated by the *in vitro* skin permeation experiment performed using the saturated solution.

ASSOCIATED CONTENT

Supporting Information

The Supporting Information is available free of charge on the ACS Publications website at DOI: 10.1021/acs.molpharmaceut.7b00926.

DOI: 10.1021/acs.molpharmaceut.7b00926
Mol. Pharmaceutics XXXX, XXX, XXX−XXX

FTIR spectra, PRX permeation profiles and retention data, and ATR-FTIR spectra (PDF)

AUTHOR INFORMATION

Corresponding Author

*Phone: +39 02 503 24635. Fax: +39 02 503 24657. E-mail: francesco.cilurzo@unimi.it.

ORCID

Pietro Matricardi: 0000-0003-2086-911X

Francesco Cilurzo: 0000-0003-3560-291X

Notes

The authors declare no competing financial interest.

ACKNOWLEDGMENTS

The authors would thank Dr. Simona Melfi for her assistance during the acquisition of the confocal images. This research was partially funded by Sapienza University, "Finanziamenti di Ateneo per la Ricerca Scientifica—Anno 2016" and Progetto di Ricerca RM11715C1743EE89.

ABBREVIATIONS USED

AFM, atomic force microscope; ATR, attenuated total reflection; CD, circular dichroism; DAPI, 4′,6-diamidino-2-phenylindole; Egg-PC, egg phosphatidylcholine; Ge, gellan; GeCh, gellan-cholesterol; GeRfv, gellan-riboflavin; J_{max}, maximal flux; MetOH, methanol; NHs, nanohydrogels; NSAIDs, nonsteroidal anti-inflammatory drugs; PDI, polydispersity index; PRX, piroxicam; Q_t, cumulative amount permeated through the skin per unit area after a period; R, electrical resistance; R_{24}, drug retained amount into the epidermis after 24 h; λ_{max}, maximum peak of absorbance

REFERENCES

(1) Chacko, R. T.; Ventura, J.; Zhuang, J.; Thayumanavan, S. Polymer nanogels: A versatile nanoscopic drug delivery platform. *Adv. Drug Delivery Rev.* **2012**, *64*, 836−851.

(2) Jiang, Y.; Chen, J.; Deng, C.; Suuronen, E. J.; Zhong, Z. Click hydrogels, microgels and nanogels: Emerging platforms for drug delivery and tissue engineering. *Biomaterials* **2014**, *35*, 4969−4985.

(3) Maya, S.; Sarmento, B.; Nair, A.; Rejinold, N. S.; Nair, S. V.; Jayakumar, R. Smart stimuli sensitive nanogels in cancer drug delivery and imaging: A review. *Curr. Pharm. Des.* **2013**, *19*, 7203−7218.

(4) Zhang, H.; Zhai, Y.; Wang, J.; Zhai, G. New progress and prospects: The application of nanogel in drug delivery. *Mater. Sci. Eng., C* **2016**, *60*, 560−568.

(5) Divya, G.; Panonnummal, R.; Gupta, S.; Jayakumar, R.; Sabitha, M. Acitretin and aloe-emodin loaded chitin nanogel for the treatment of psoriasis. *Eur. J. Pharm. Biopharm.* **2016**, *107*, 97−109.

(6) Kim, J.; Gauvin, R.; Yoon, H. J.; Kim, J. H.; Kwon, S. M.; Park, H. J.; Baek, S. H.; Cha, J. M.; Bae, H. Skin penetration-inducing gelatin methacryloyl nanogels for transdermal macromolecule delivery. *Macromol. Res.* **2016**, *24* (12), 1115−1125.

(7) Panonnummal, R.; Jayakumar, R.; Sabitha, M. Comparative anti-psoriatic efficacy studies of clobetasol loaded chitin nanogel and marketed cream. *Eur. J. Pharm. Sci.* **2017**, *96*, 193−206.

(8) Zabihi, F.; Wieczorek, S.; Dimde, M.; Hedtrich, S.; Borner, H. G.; Haag, R. Intradermal drug delivery by nanogel-peptide conjugates; specific and efficient transportation of temoporfin. *J. Controlled Release* **2016**, *242*, 35−41.

(9) Šmejkalová, D.; Muthný, T.; Nešporová, K.; Hermannová, M.; Achbergerová, E.; Huerta-Angeles, G.; Svoboda, M.; Čepa, M.; Machalová, V.; Luptáková, D.; Velebny, V. Hyaluronan polymeric micelles for topical drug delivery. *Carbohydr. Polym.* **2017**, *156*, 86−96.

(10) Abioye, A. O.; Issah, S.; Kola-Mustapha, A. Ex vivo skin permeation and retention studies on chitosan−ibuprofen−gellan ternary nanogel prepared by in situ ionic gelation technique—a tool for controlled transdermal delivery of ibuprofen. *Int. J. Pharm.* **2015**, *490*, 112−130.

(11) Samah, N. H. A.; Heard, C. M. Enhanced in vitro transdermal delivery of caffeine using a temperature- and pH-sensitive nanogel, poly(NIPAM-co-AAc). *Int. J. Pharm.* **2013**, *453*, 630−640.

(12) Rancan, F.; Asadian-Birjand, M.; Dogan, S.; Graf, C.; Cuellar, L.; Lommatzsch, S.; Blume-Peytavi, U.; Calderón, M.; Vogt, A. Effects of thermoresponsivity and softness on skin penetration and cellular uptake of polyglycerol-based nanogels. *J. Controlled Release* **2016**, *228*, 159−169.

(13) D'Arrigo, G.; Navarro, G.; Di Meo, C.; Matricardi, P.; Torchilin, V. Gellan gum nanohydrogel containing anti-inflammatory and anti-cancer drugs: a multi-drug delivery system for a combination therapy in cancer treatment. *Eur. J. Pharm. Biopharm.* **2014**, *87* (1), 208−216.

(14) Montanari, E.; De Rugeriis, M. C.; Di Meo, C.; Censi, R.; Coviello, T.; Alhaique, F.; Matricardi, P. One-step formation and sterilization of gellan and hyaluronan nanohydrogels using autoclave. *J. Mater. Sci.: Mater. Med.* **2015**, *26*, 32.

(15) Di Meo, C.; Montanari, E.; Manzi, L.; Villani, C.; Coviello, T.; Matricardi, P. Highly versatile nanohydrogel platform based on riboflavin-polysaccharide derivatives useful in the development of intrinsically fluorescent and cytocompatible drug carriers. *Carbohydr. Polym.* **2015**, *115*, 502−509.

(16) Montanari, E.; Di Meo, C.; Sennato, S.; Francioso, A.; Marinelli, A. L.; Ranzo, F.; Schippa, S.; Coviello, T.; Bordi, F.; Matricardi, P. Hyaluronan-cholesterol nanohydrogels: Characterisation and effectiveness in carrying alginate lyase. *New Biotechnol.* **2017**, *37*, 80−89.

(17) Cilurzo, F.; Gennari, C. G. M.; Selmin, F.; Franzè, S.; Musazzi, U. M.; Minghetti, P. On the characterization of medicated plasters containing NSAIDs according to novel indications of USP and EMA: adhesive property and in vitro skin permeation studies. *Drug Dev. Ind. Pharm.* **2015**, *41*, 183−189.

(18) Campione, E.; Diluvio, L.; Paternò, E. J.; Chimenti, S. Topical Treatment of Actinic Keratoses with Piroxicam 1% Gel. *Am. J. Clin Derm* **2010**, *11*, 45−50.

(19) Campione, E.; Paterno, E. J.; Candi, E.; Falconi, M.; Costanza, G.; Diluvio, L.; Terrinoni, A.; Bianchi, L.; Orlandi, A. The relevance of piroxicam for the prevention and treatment of nonmelanoma skin cancer and its precursors. *Drug Des., Dev. Ther.* **2015**, *9*, 5843−5850.

(20) Henry, D.; McGettigan, P. Epidemiology overview of gastrointestinal and renal toxicity of NSAIDs. *Int. J. Clin. Pract., Suppl.* **2003**, *135*, 43−49.

(21) Laporte, J. R.; Ibanez, L.; Vidal, X.; Vendrell, L.; Leone, R. Upper gastrointestinal bleeding associated with the use of NSAIDs: newer versus older agents. *Drug Saf.* **2004**, *27*, 411−420.

(22) Godwin, D. A.; Kim, N. H.; Felton, L. A. Influence of Transcutol® CG on the skin accumulation and transdermal permeation of ultraviolet absorbers. *Eur. J. Pharm. Biopharm.* **2002**, *53* (1), 23−27.

(23) D'Arrigo, G.; Di Meo, C.; Gaucci, E.; Chichiarelli, S.; Coviello, T.; Capitani, D.; Alhaique, F.; Matricardi, P. Self-assembled gellan-based nanohydrogels as a tool for prednisolone delivery. *Soft Matter* **2012**, *8*, 11557−11564.

(24) Franzé, S.; Donadoni, G.; Podestà, A.; Procacci, P.; Orioli, M.; Carini, M.; Minghetti, P.; Cilurzo, F. Tuning the extent and depth of penetration of flexible liposomes in human skin. *Mol. Pharmaceutics* **2017**, *14* (6), 1998−2009.

(25) Musazzi, U. M.; Matera, C.; Dallanoce, C.; Vacondio, F.; De Amici, M.; Vistoli, G.; Cilurzo, F.; Minghetti, P. On the selection of an opioid for local skin analgesia: Structure-skin permeability relationships. *Int. J. Pharm.* **2015**, *489*, 177−185.

(26) Franzé, S.; Gennari, C. G. M.; Minghetti, P.; Cilurzo, F. Influence of chemical and structural features of low molecular weight heparins (LMWHs) on skin penetration. *Int. J. Pharm.* **2015**, *481* (1−2), 79−83.

DOI: 10.1021/acs.molpharmaceut.7b00926
Mol. Pharmaceutics XXXX, XXX, XXX−XXX

(27) Selmin, F.; Cilurzo, F.; Aluigi, A.; Franzè, S.; Minghetti, P. Regenerated keratin membrane to match the in vitro drug diffusion through human epidermis. *Results Pharma Sci.* **2012**, *2* (1), 72−78.
(28) Rozou, S.; Voulgari, A.; Antoniadou-Vyza, E. The effect of pH dependent molecular conformation and dimerization phenomena of piroxicam on the drug: cyclodextrin complex stoichiometry and its chromatographic behaviour. A new specific HPLC method for piroxicam:cyclodextrin formulations. *Eur. J. Pharm. Sci.* **2004**, *21*, 661−669.
(29) Tsai, R.-S.; Carrupt, P.-A.; Tayar, N. E.; Giroud, Y.; Andrade, P.; Testa, B.; Brée, F.; Tillement, J.-P. Physicochemical and structural properties of non-steroidal anti-inflammatory oxicams. *Helv. Chim. Acta* **1993**, *76*, 842−854.
(30) Hendrickson, G. R.; Lyon, L. A. Microgel translocation through pores under confinement. *Angew. Chem., Int. Ed.* **2010**, *49*, 2193−2197.
(31) Campani, V.; Biondi, M.; Mayol, L.; Cilurzo, F.; Franzé, S.; Pitaro, M.; De Rosa, G. Nanocarriers to Enhance the Accumulation of Vitamin K1 into the Skin. *Pharm. Res.* **2016**, *33* (4), 893−908.
(32) Karande, P.; Jain, A.; Ergun, K.; Kispersky, V.; Mitragotri, S. Design principles of chemical penetration enhancers for transdermal drug delivery. *Proc. Natl. Acad. Sci. U. S. A.* **2005**, *102* (13), 4688−93.
(33) Gennari, C. G. M.; Franzè, S.; Pellegrino, S.; Corsini, E.; Vistoli, G.; Montanari, L.; Minghetti, P.; Cilurzo, F. Skin Penetrating Peptide as a Tool to Enhance the Permeation of Heparin through Human Epidermis. *Biomacromolecules* **2016**, *17* (1), 46−55.
(34) Cilurzo, F.; Selmin, F.; Gennari, C. G. M.; Montanari, L.; Minghetti, P. Application of methyl methacrylate copolymers to the development of transdermal or loco-regional drug delivery systems. *Expert Opin. Drug Delivery* **2014**, *11* (7), 1033−1045.
(35) Damien, F.; Boncheva, M. The extent of orthorhombic lipid phases in the stratum corneum determines the barrier efficiency of human skin in vivo. *J. Invest. Dermatol.* **2010**, *130*, 611−614.
(36) Cilurzo, F.; Vistoli, G.; Gennari, C.; Selmin, F.; Gardoni, F.; Franzè, S.; Campisi, M.; Minghetti, P. The role of the conformational profile of polysaccharides on skin penetration: the case of hyaluronan and sulfates thereof. *Chem. Biodiversity* **2014**, *11* (3), 551−561.
(37) Musazzi, U. M.; Santini, B.; Selmin, F.; Marini, V.; Corsi, F.; Allevi, R.; Ferretti, A. M.; Prosperi, D.; Cilurzo, F.; Colombo, M.; Minghetti, P. Impact of semi-solid formulations on skin penetration of iron oxide nanoparticles. *J. Nanobiotechnol.* **2017**, *15*, 14−20.
(38) Cosco, D.; Celia, C.; Cilurzo, F.; Trapasso, E.; Paolino, D. Colloidal carriers for the enhanced delivery through the skin. *Expert Opin. Drug Delivery* **2008**, *5* (5), 737−755.
(39) Campani, V.; Biondi, M.; Mayol, L.; Cilurzo, F.; Pitaro, M.; De Rosa, G. Development of nanoemulsions for topical delivery of vitamin K1. *Int. J. Pharm.* **2016**, *511*, 170−177.

DOI: 10.1021/acs.molpharmaceut.7b00926
Mol. Pharmaceutics XXXX, XXX, XXX−XXX